Supporting Information

Nanocomposites of Ag_3PO_4 and Phosphorous-Doped Graphitic Carbon Nitride for Ketamine Removal

Changsheng Guo, [†, ※] Miao Chen, [†, ‡, ※] Linlin Wu, [†] Yingying Pei, [†] Chunhua Hu, [‡] Yuan Zhang, [†] and Jian Xu [†, *]

[†] State Key Laboratory of Environmental Criteria and Risk Assessment, Chinese Research Academy of Environmental Sciences, Beijing, 100012, China

[‡] Key Laboratory of Poyang Lake Environment and Resource Utilization, Ministry of Education, School of Resources Environmental and Chemical Engineering, Nanchang University, Nanchang, 330031, China

[*] Corresponding author, Email: xujian@craes.org.cn (J. Xu)

※ The first two authors contributed equally to this work.

(Text S1 ~ Text S3)

(Figure S1 ~ Figure S10)

(Table S1 ~ Table S4)

Additional Details on Analytical Methods

Text S1. Measurement of KET concentration

The concentration of KET was quantified by UPLC-MS/MS, which was consisted of a Xevo TQ-S triple quadrupole mass spectrometer (Waters, MA, USA) and a Waters ACQUITY liquid chromatography. The MS was in a multiple-reaction monitoring (MRM) mode with an electrospray ionization (ESI) in the positive mode. A Waters C 18 column (50 mm×2.1 mm, 1.7 μm) maintained at 40°C was used to guarantee the separation of target compounds. Milli Q water containing 0.1% formic acid (v/v) (phase A) and acetonitrile (phase B) were used as the mobile phase. The gradient elution condition was as follows: 0 ~ 0.5 min, 10% B; 0.5 ~ 3 min, 10% ~ 40% B; 3.0 ~ 3.2 min, 40% ~ 95% B; 3.2 ~ 4.0 min, 95% B; 4.0 ~ 4.2 min, 95% ~ 10% B, 4.2 ~ 5.7 min, 10%B. The retention time of KET was 1.52 min. The sample injection volume was set at 5 μL and the flow rate of mobile phase was 0.45 mL·min^{-1}. The mass spectrometer conditions were as follows: Capillary voltage was 670 V, desolvation temperature was 450°C, and source gas flow was 1000 (L/Hr).

Text S2. Identification of KET intermediates

KET intermediates were identified by a Thermo Scientific Q Exactive LC-MS system (Thermo fisher, USA), which was equipped with a C18 column (100×2.1 mm, 5μm, Hypersil GOLD, USA). An ESI source in positive mode was used and a full mass scan mode was carried out to detect the intermediates, with the scanning range of m/z 50 ~ 500. Acetonitrile and Milli Q water with 0.1% formic acid (v/v) were used as the mobile phase

A and B, respectively, and the mobile phase flow rate was 0.2 mL·min^{-1}. The gradient elution program was as follows: 0 ~ 2 min, 10% A; 2 ~ 30 min, 10% ~ 95% A; 30 ~ 35 min, 95% A; 35 ~ 40 min, 95% ~ 10% A; 40 ~ 45 min, 10% A. The column temperature was 35°C and the injection volume was 20 μL. The capillary voltage was 3 kV, and the drying gas temperature was 320°C.

Text S3. Detection of ·OH and ·O_2^- by Electron spin resonance (ESR) technique

The reactive species of ·OH and ·O_2^- were investigated by a Magnet Tech MS400 spectrometer with that 5,5-dimethyl-1-pyrroline-N-oxide (DMPO) was used as the spin trap. A 300 W Xenon lamp (Institute of Electric Light Source, Beijing) was used as the simulated visible light. ESR spectra of P-g-C_3N_4 and Ag_3PO_4/P-g-C_3N_4 (1:1) were investigated in darkness and under visible light irradiation. The generation of ·OH and ·O_2^- were detected in deionized water and methanol, respectively.

Figure S1. SEM images of the synthesized samples. (a) P-g-C_3N_4; (b) A/CN (1:2); (c) A/CN (1:1); (d) A/CN (2:1); (e) A/CN (10:1); (f) Ag_3PO_4.

Figure S2. SEM image of A/CN (1:1) (a), and corresponding energy-dispersive X-ray spectroscopy (EDX) elemental analysis spectrum for C (b), N (c), O (d), P (e), Ag (f).

Figure S3. HRTEM images of A/CN (1:1) composite.

Figure S4. N_2 adsorption-desorption isotherms and the corresponding pore size distribution curve (inside).

Figure S5. PL spectra (a) and transient photocurrent responses (b) of the synthesized samples.

Figure S6. The pseudo-first-order plots of -ln (C_t/C_0) vs. time of KET degradation at different pH value (a) and in the presence of HOC_3^- (b); DOM (c) and NO_3^- (d).

Figure S7. PL spectra observed during irradiation of A/CN (1:1) in TA solution (a) and absorbance spectra observed during irradiation of A/CN (1:1) in NBT solution (b).

Figure S8. ESR signals of DMPO adduct with ·OH (a-b) and $\cdot O_2^-$ (c-d) in the suspension of P-g-C_3N_4 (a, c) and A/CN (1:1) (b, d) with or without visible light irradiation.

Figure S9. LC-MS/MS total ion chromatograms of KET at different time. (a) 2 min; (b) 10 min; (c) 15 min; (d) 30 min; (e) 45 min. (Conditions: $[KET]_0$=10 mg/L; $[catalyst]_0$=1g/L).

Figure S10. Mass spectra detected during the photodegradation of KET by Ag_3PO_4/P-g-C_3N_4 composite under visible light irradiation.

Table S1. The dosage of reagents used for the preparation of Ag_3PO_4 and Ag_3PO_4/P-g-C_3N_4.

Table S2. Electrical energy per order of the synthesized samples.

Table S3. Water quality parameters of different water matrices.

Table S4. The possible degradation intermediates of KET over Ag_3PO_4/P-g-C_3N_4 composite under visible light irradiation.

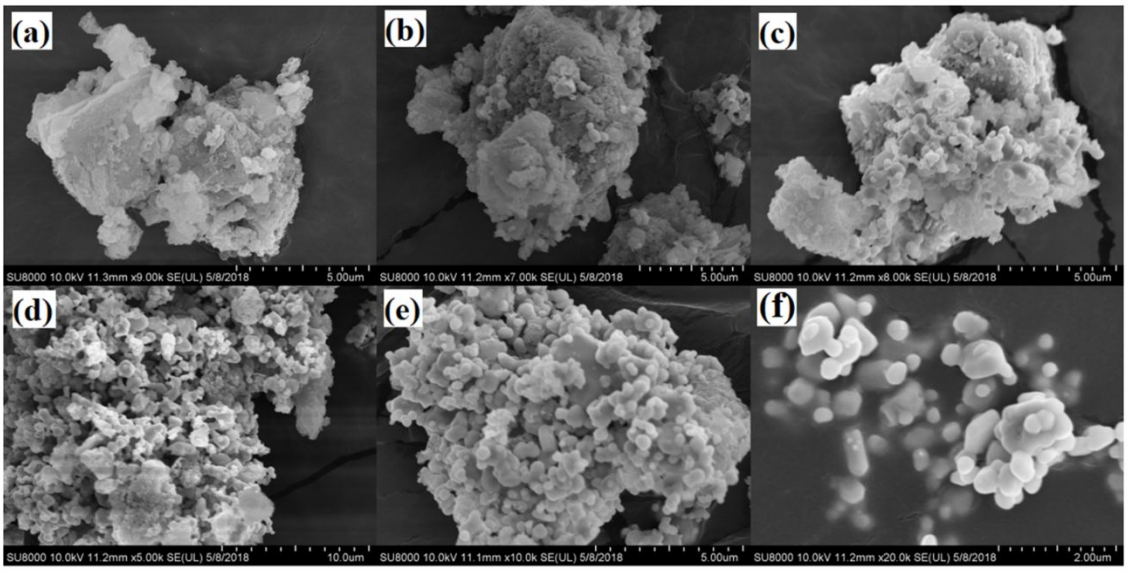

Figure S1. SEM images of the synthesized samples. (a) P-g-C_3N_4; (b) A/CN (1:2); (c) A/CN (1:1); (d) A/CN (2:1); (e) A/CN (10:1); (f) Ag_3PO_4.

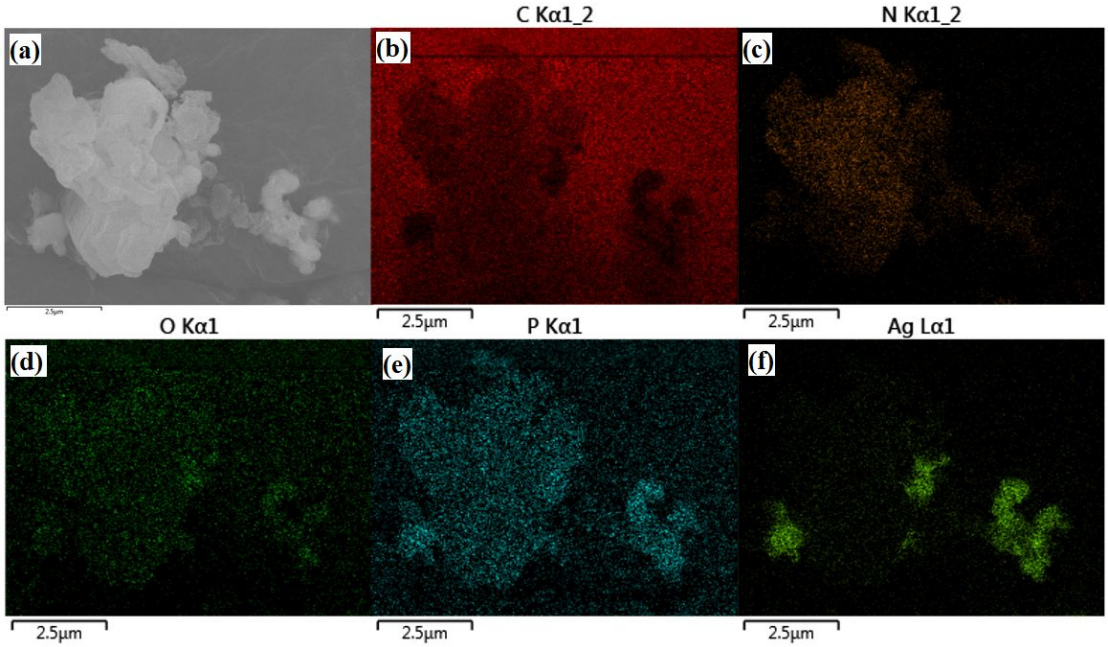

Figure S2. SEM image of A/CN (1:1) (a), and corresponding energy-dispersive X-ray spectroscopy (EDX) elemental analysis spectrum for C (b), N (c), O (d), P (e), Ag (f).

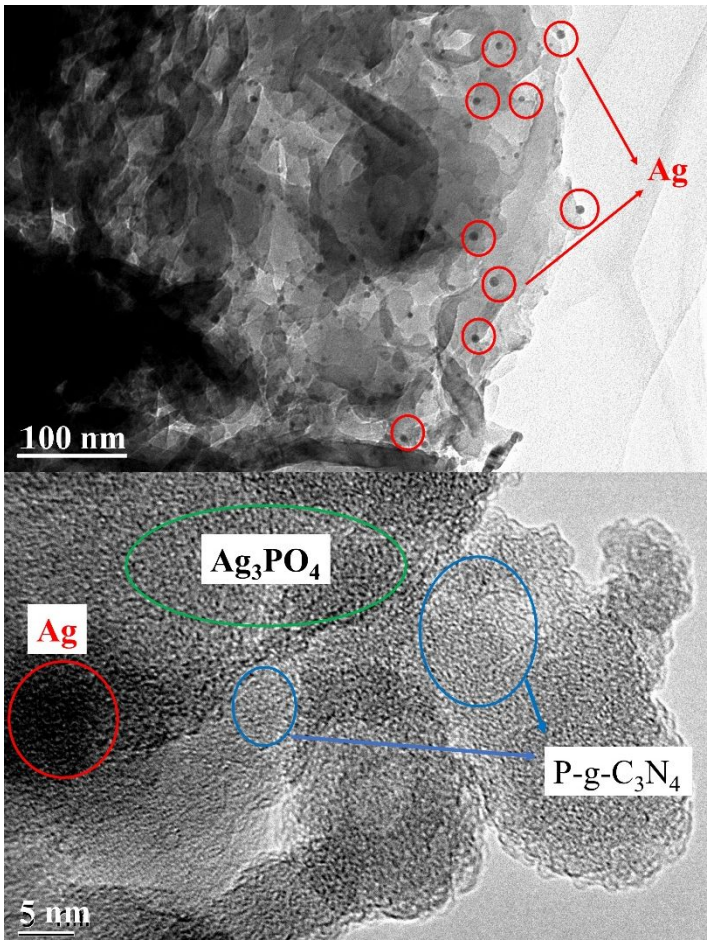

Figure S3. HRTEM images of A/CN (1:1) composite.

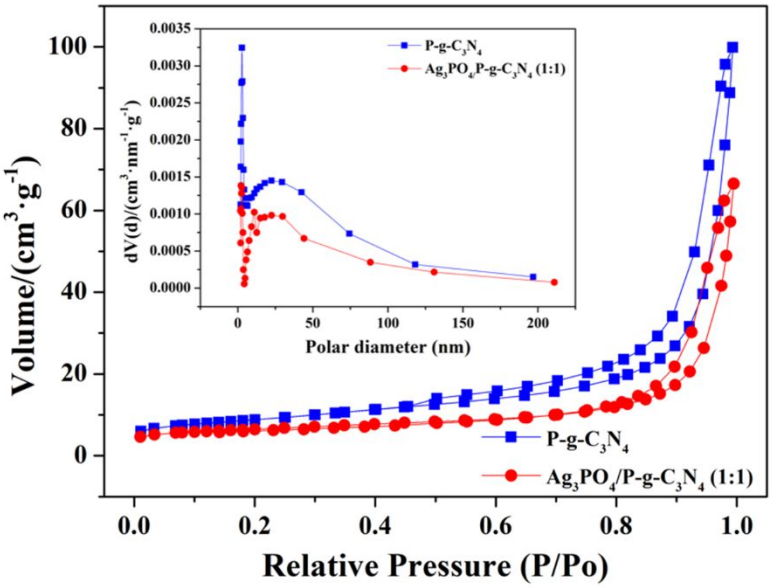

Figure S4. N_2 adsorption-desorption isotherms and the corresponding pore size distribution curve (inside).

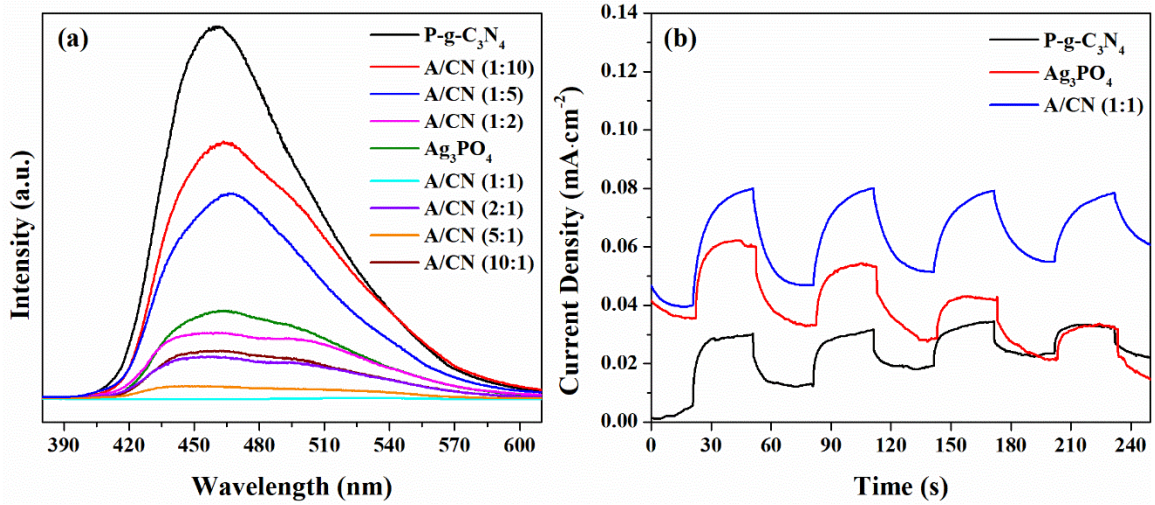

Figure S5. PL spectra (a) and transient photocurrent responses (b) of the synthesized samples.

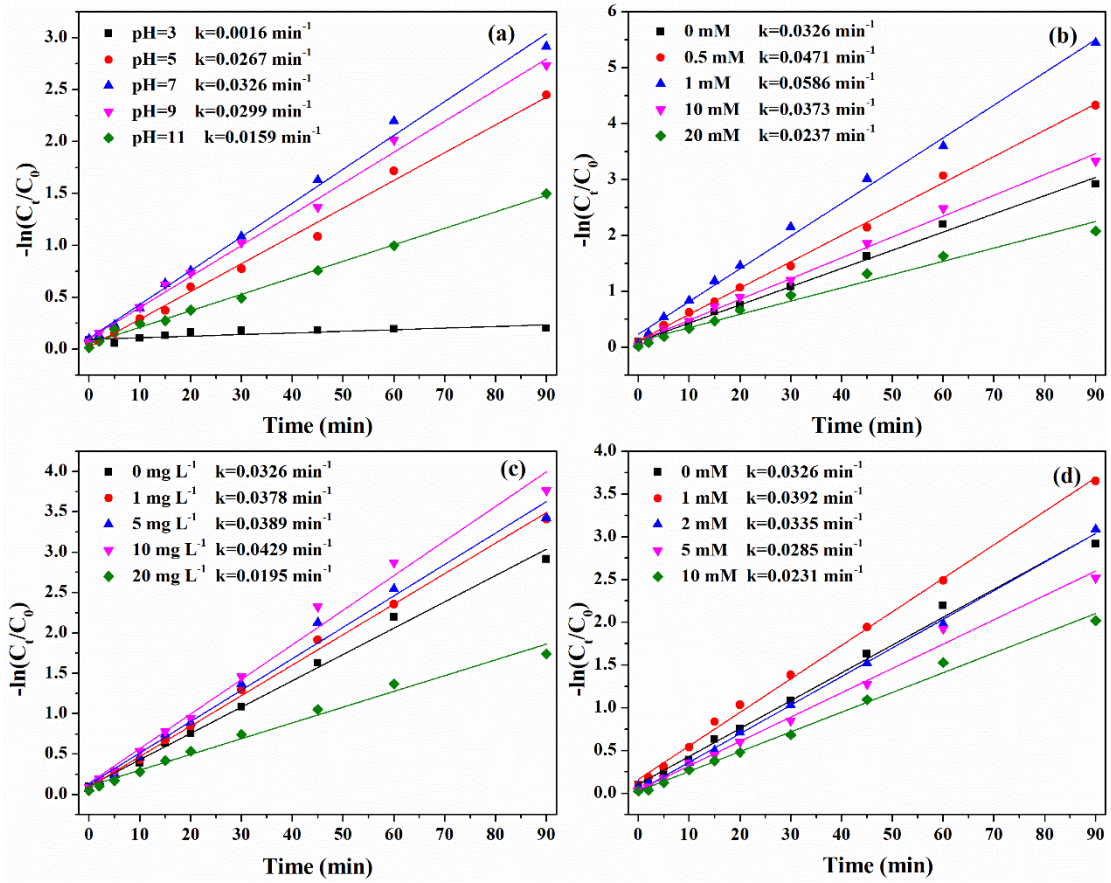

Figure S6. The pseudo-first-order plots of -ln (C_t/C_0) vs. time of KET degradation at different pH value (a) and in the presence of HCO_3^- (b); DOM (c) and NO_3^- (d).

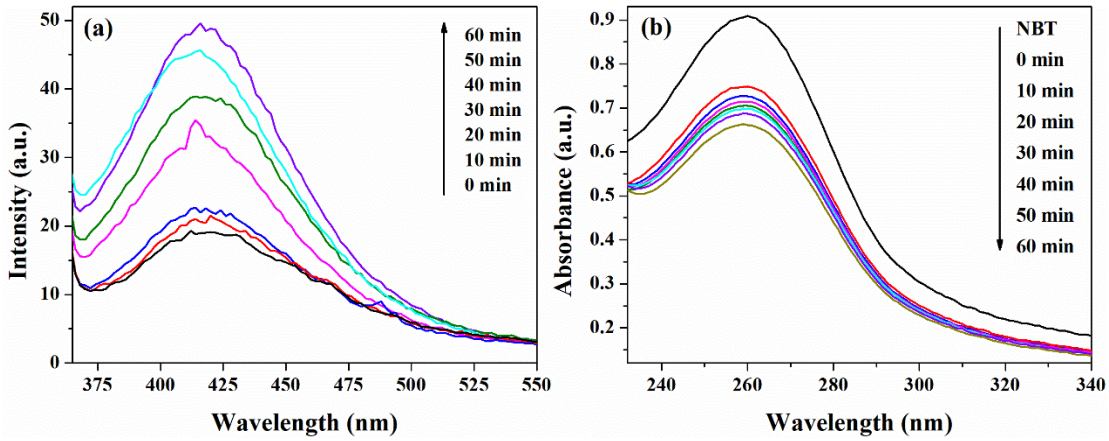

Figure S7. PL spectrum observed during irradiation of A/CN (1:1) in TA solution (a) and absorbance spectrum observed during irradiation of A/CN (1:1) in NBT solution (b).

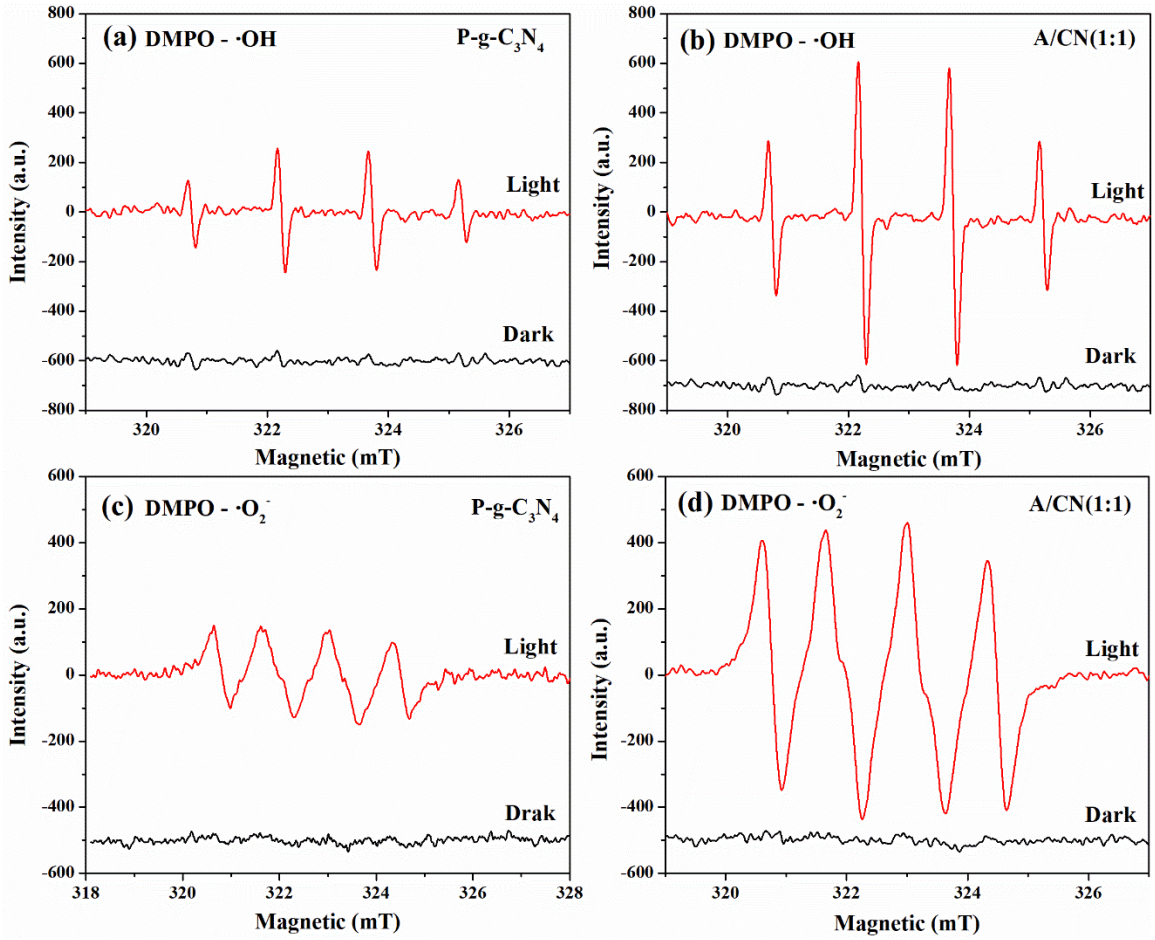

Figure S8. ESR signals of DMPO adduct with ·OH (a-b) and $\cdot O_2^-$ (c-d) in the suspension of P-g-C_3N_4 (a, c) and A/CN (1:1) (b, d) with or without visible light irradiation.

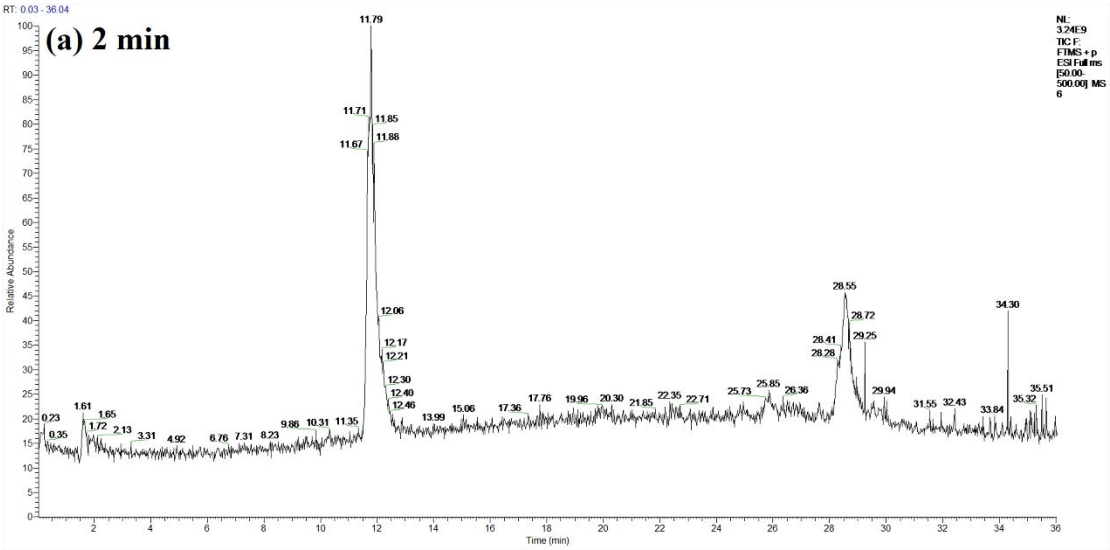
RT: 0.03 - 36.04
(a) 2 min
NL:
3.24E9
TIC F:
FTMS + p
ESI Full ms
[50.00-
500.00] MS
6
Relative Abundance
Time (min)

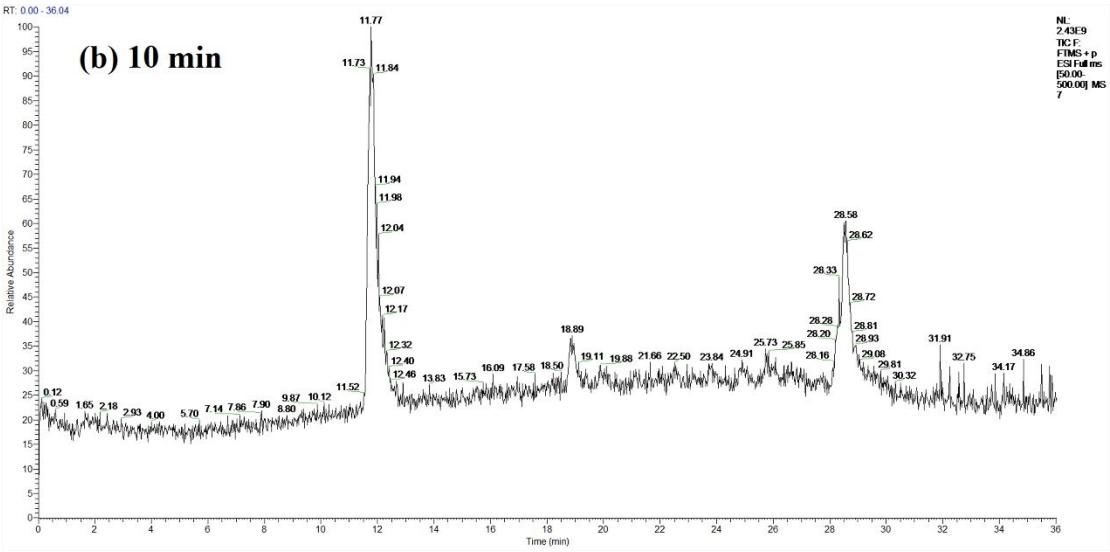
RT: 0.00 - 36.04
(b) 10 min
NL:
2.43E9
TIC F:
FTMS + p
ESI Full ms
[50.00-
500.00] MS
7
Relative Abundance
Time (min)

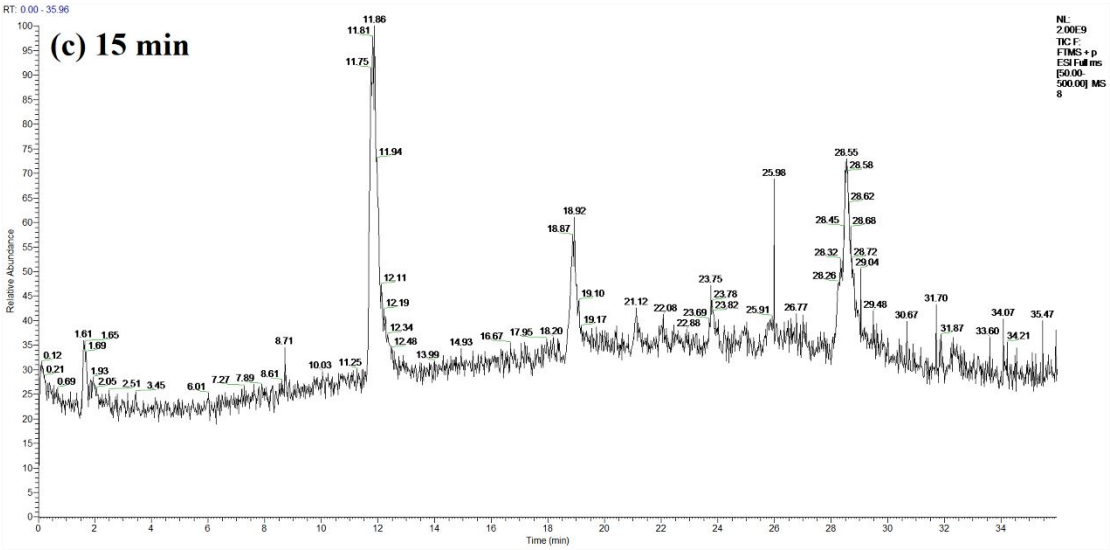
(c) 15 min
RT: 0.00 - 35.96
NL:
2.00E9
TIC F:
FTMS + p
ESI Full ms
[50.00-
500.00] MS
8
Relative Abundance
Time (min)

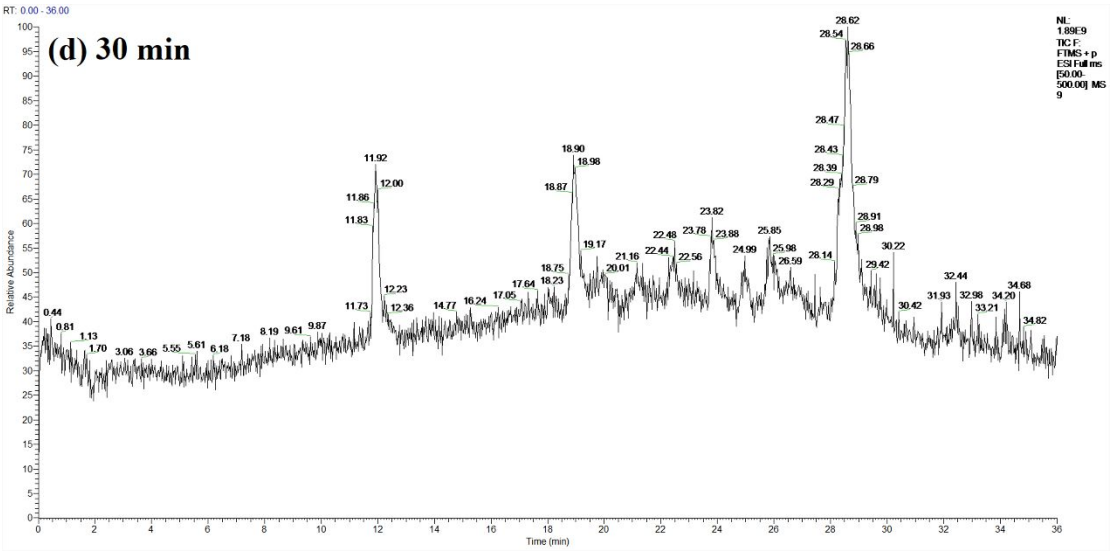
(d) 30 min
RT: 0.00 - 36.00
NL:
1.89E9
TIC F:
FTMS + p
ESI Full ms
[50.00-
500.00] MS
9
Relative Abundance
Time (min)

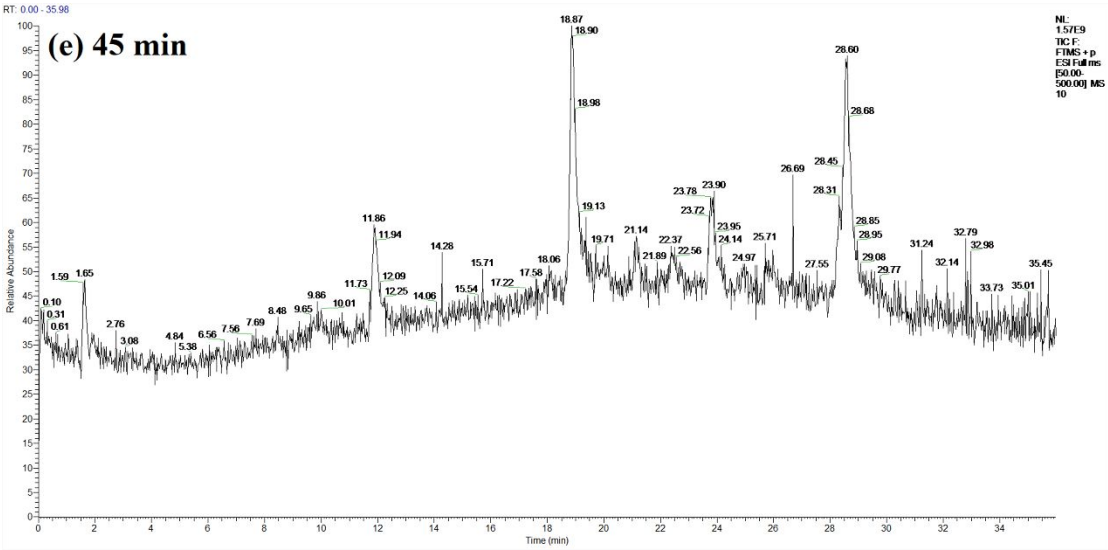

Figure S9. LC-MS/MS total ion chromatograms of KET at different time. (a) 2 min; (b) 10 min; (c) 15 min; (d) 30 min; (e) 45 min. (Conditions: $[KET]_0$=10 mg·L^{-1}; $[catalyst]_0$=1g·L^{-1}).

P1 m/z 224; P2 m/z 222

10 #2337-2354 RT: 22.35-22.50 AV: 9 SB: 2 22.61 , 22.65 NL: 2.83E7
T: FTMS + p ESI Full ms [50.00-500.00]

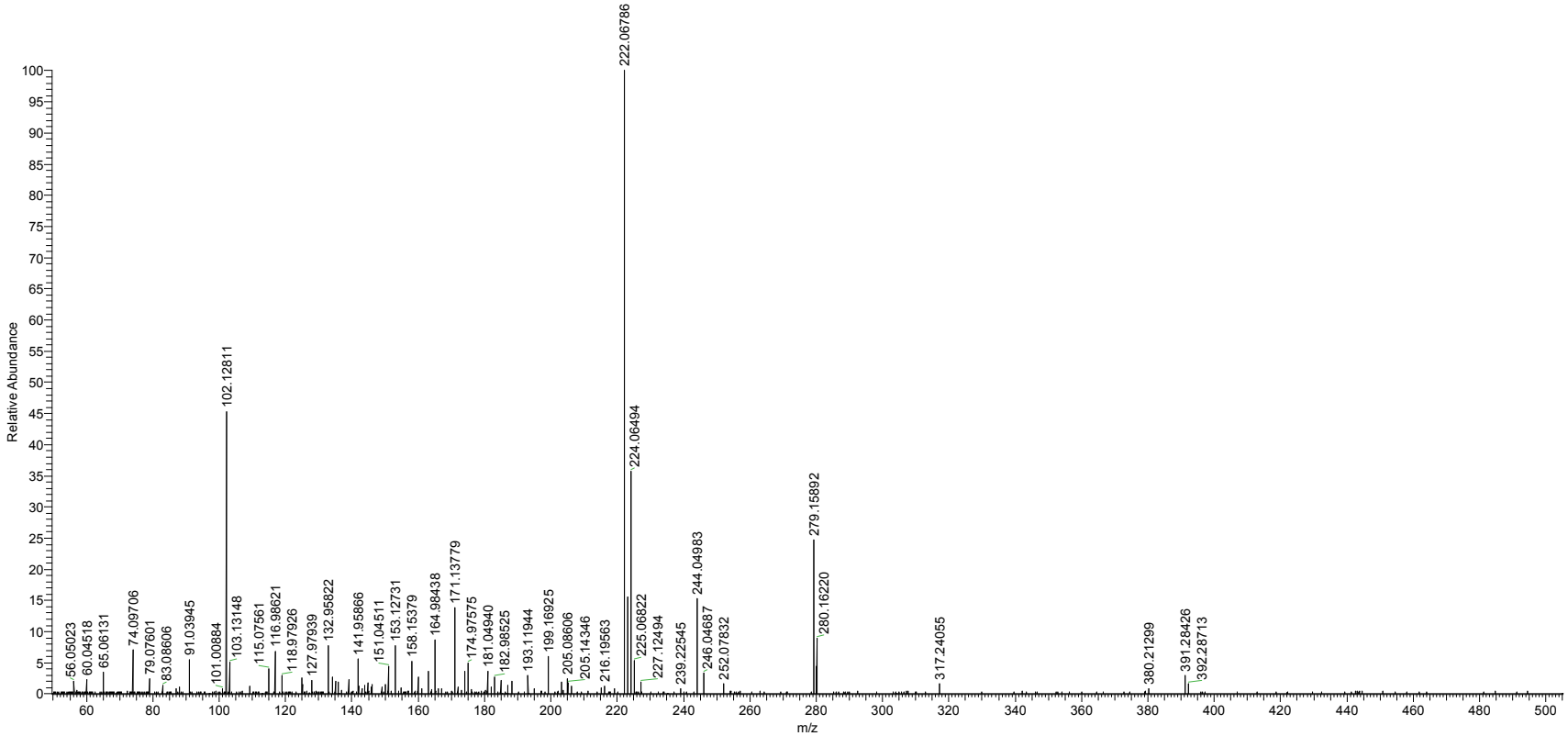

P3 m/z 236

10 #2478-2501 RT: 23.71-23.92 AV: 12 SB: 51 22.49-22.85 , 24.57-25.16 NL: 1.41E8
T: FTMS + p ESI Full ms [50.00-500.00]

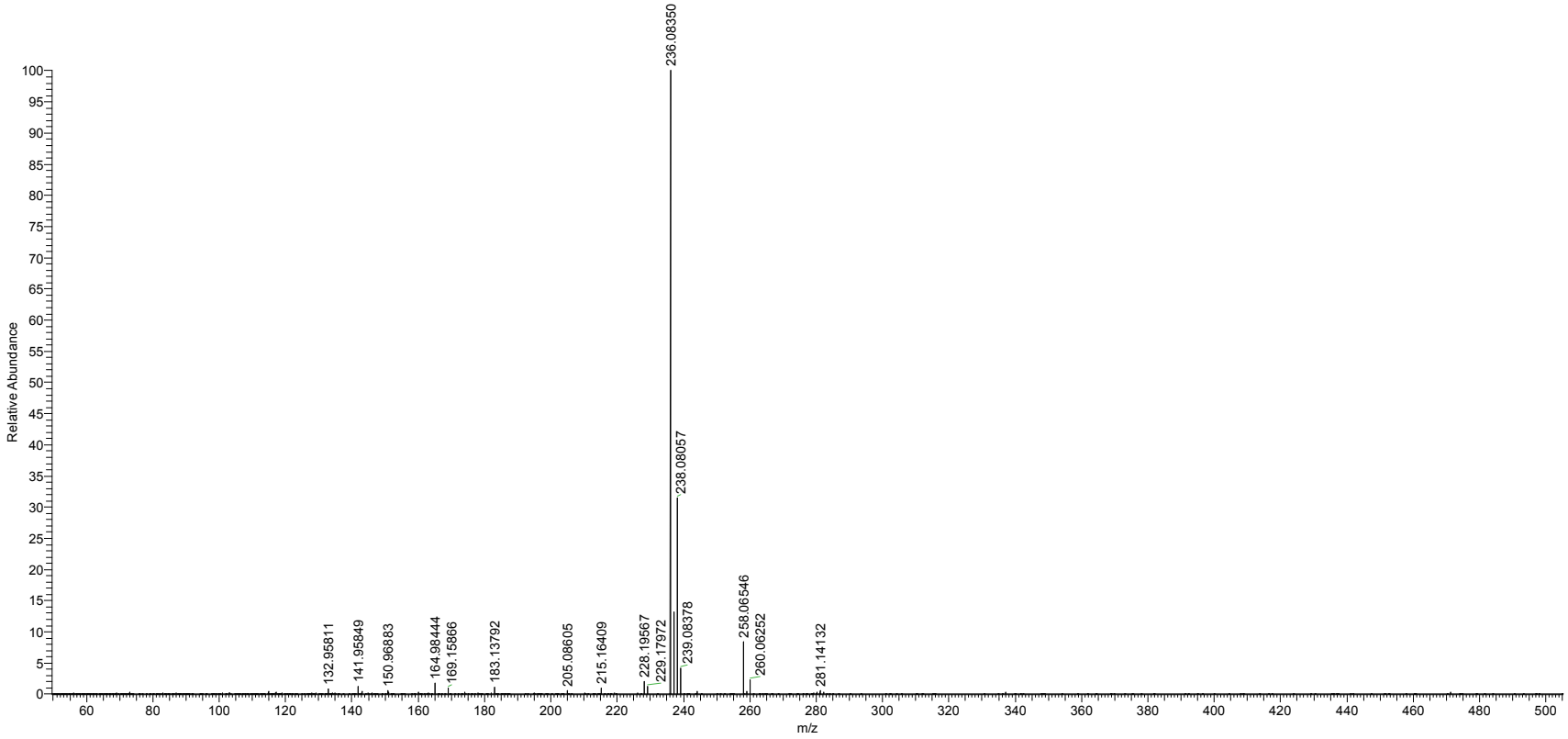

P4 m/z 254; P5 m/z 256

10 #1963-1989 RT: 18.77-19.02 AV: 14 SB: 96 16.63-17.59 , 19.57-20.43 NL: 3.68E8
T: FTMS + p ESI Full ms [50.00-500.00]

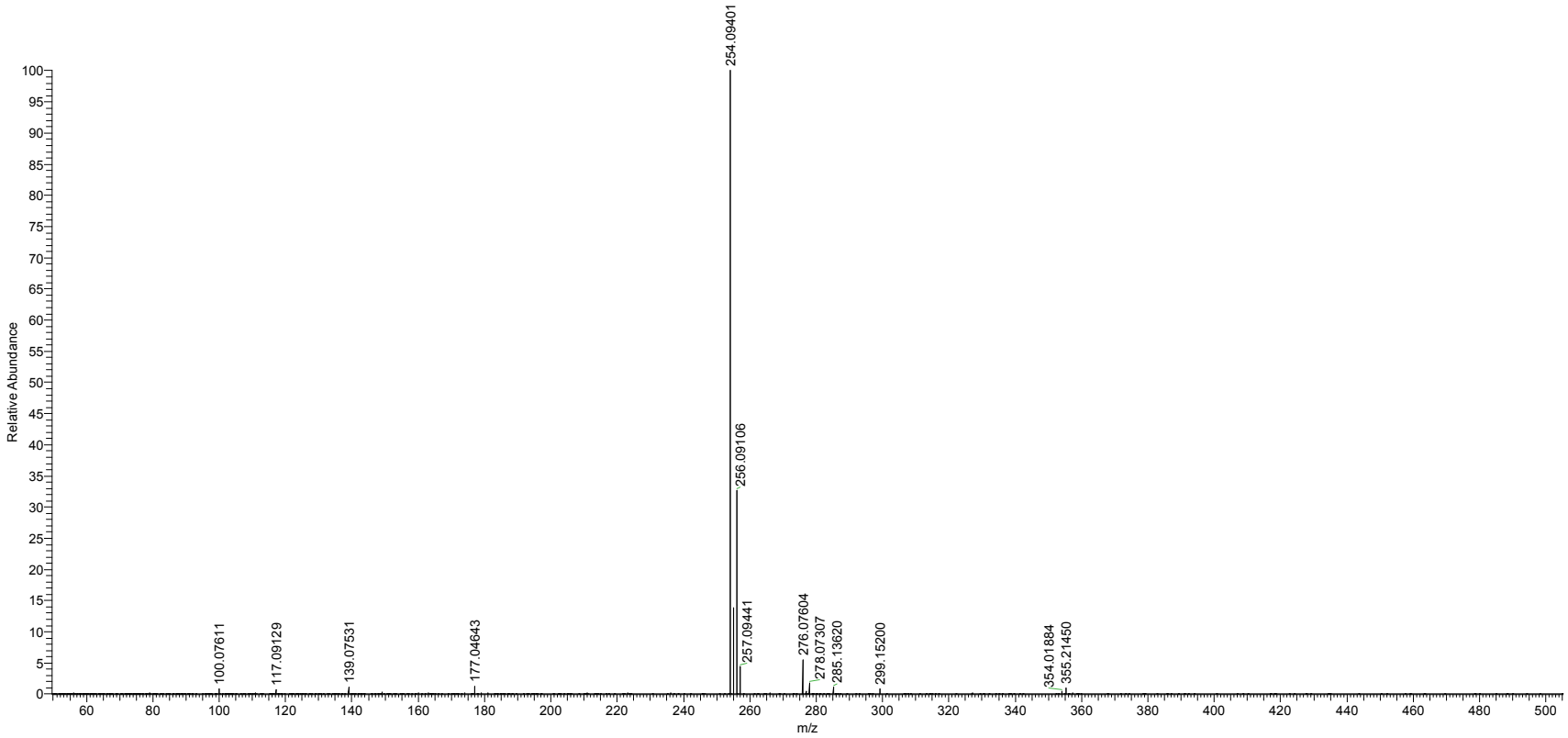

P6 m/z 200

10 #2689-2729 RT: 25.71-26.10 AV: 21 SB: 71 24.51-25.12 , 26.33-27.04 NL: 2.58E7
T: FTMS + p ESI Full ms [50.00-500.00]

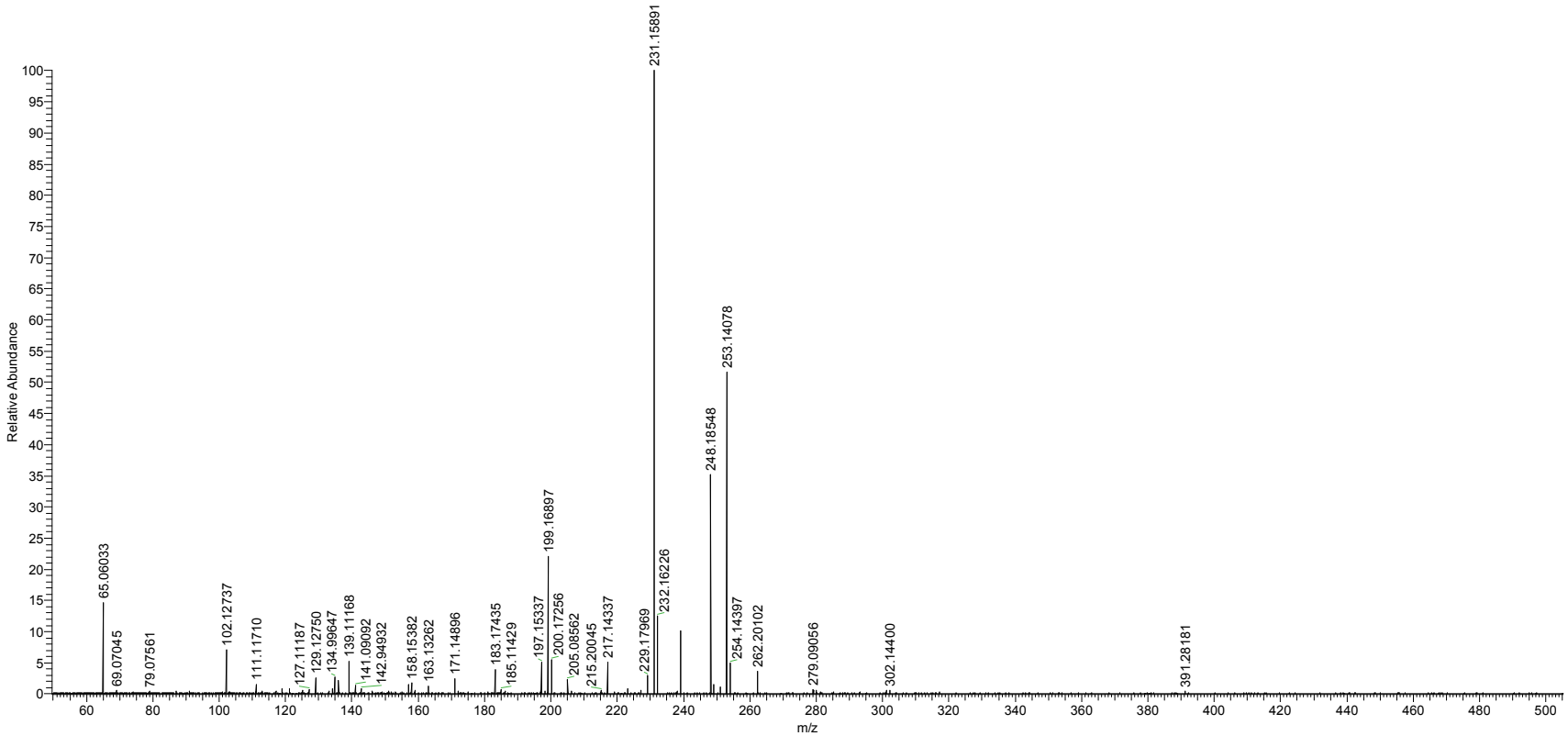

P7 m/z 240; P11 m/z 241

10 #1232-1274 RT: 11.79-12.17 AV: 21 SB: 86 9.65-10.47 , 12.47-13.28 NL: 1.13E8
T: FTMS + p ESI Full ms [50.00-500.00]

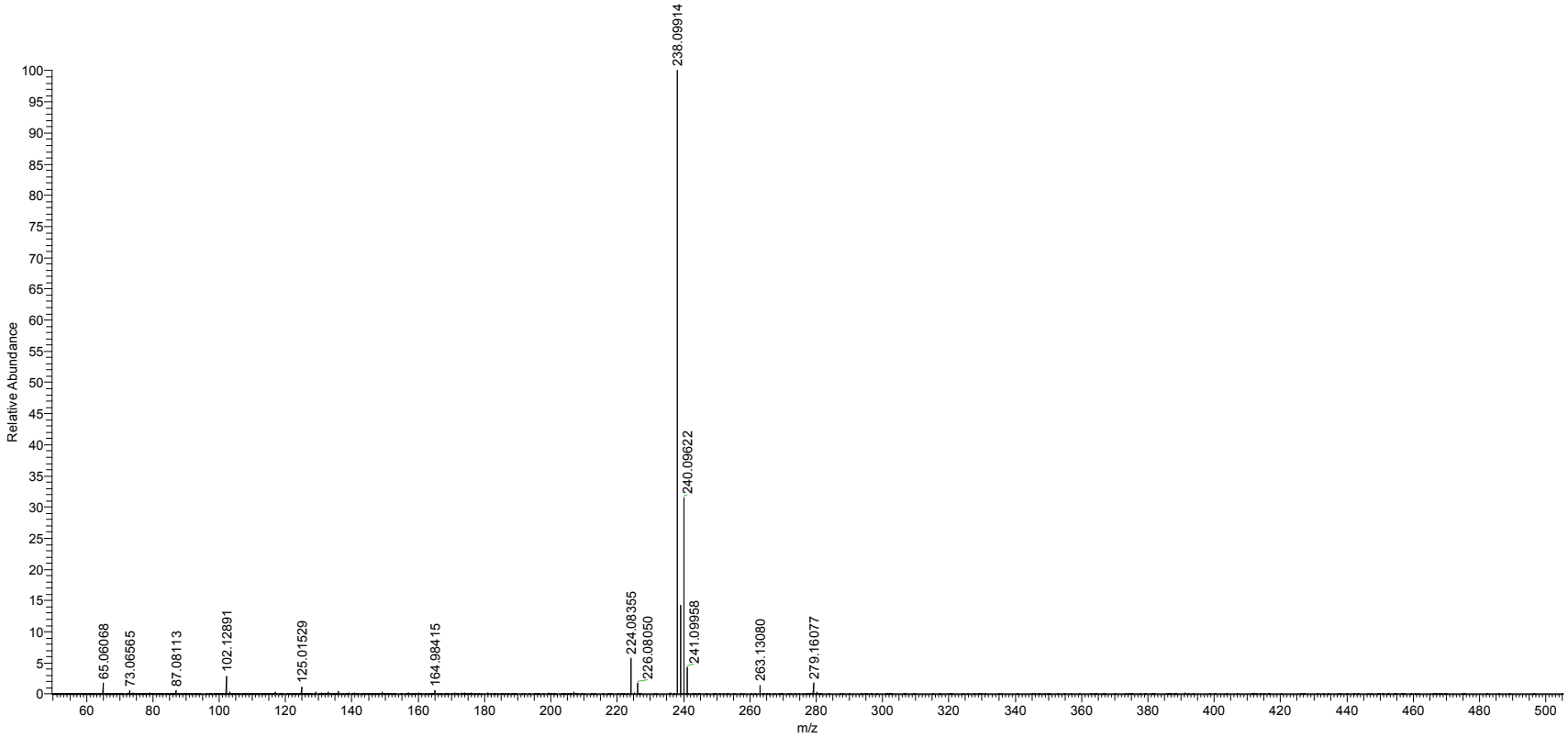

P8 m/z 225; P9 m/z 226; P10 m/z 243

10 #2198-2226 RT: 21.03-21.28 AV: 14 SB: 68 19.59-20.35 , 21.61-22.14 NL: 3.17E7
T: FTMS + p ESI Full ms [50.00-500.00]

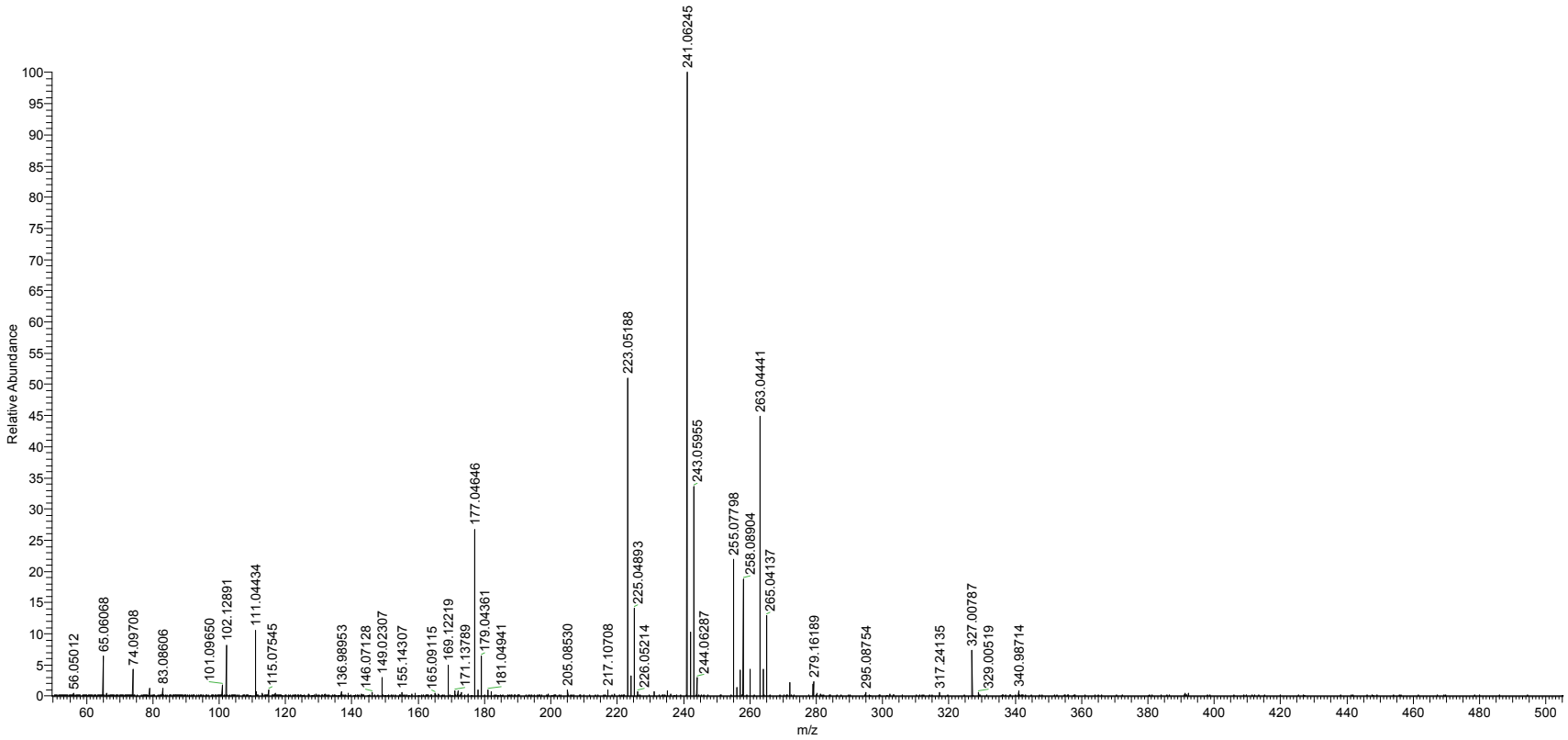

P12 m/z 279

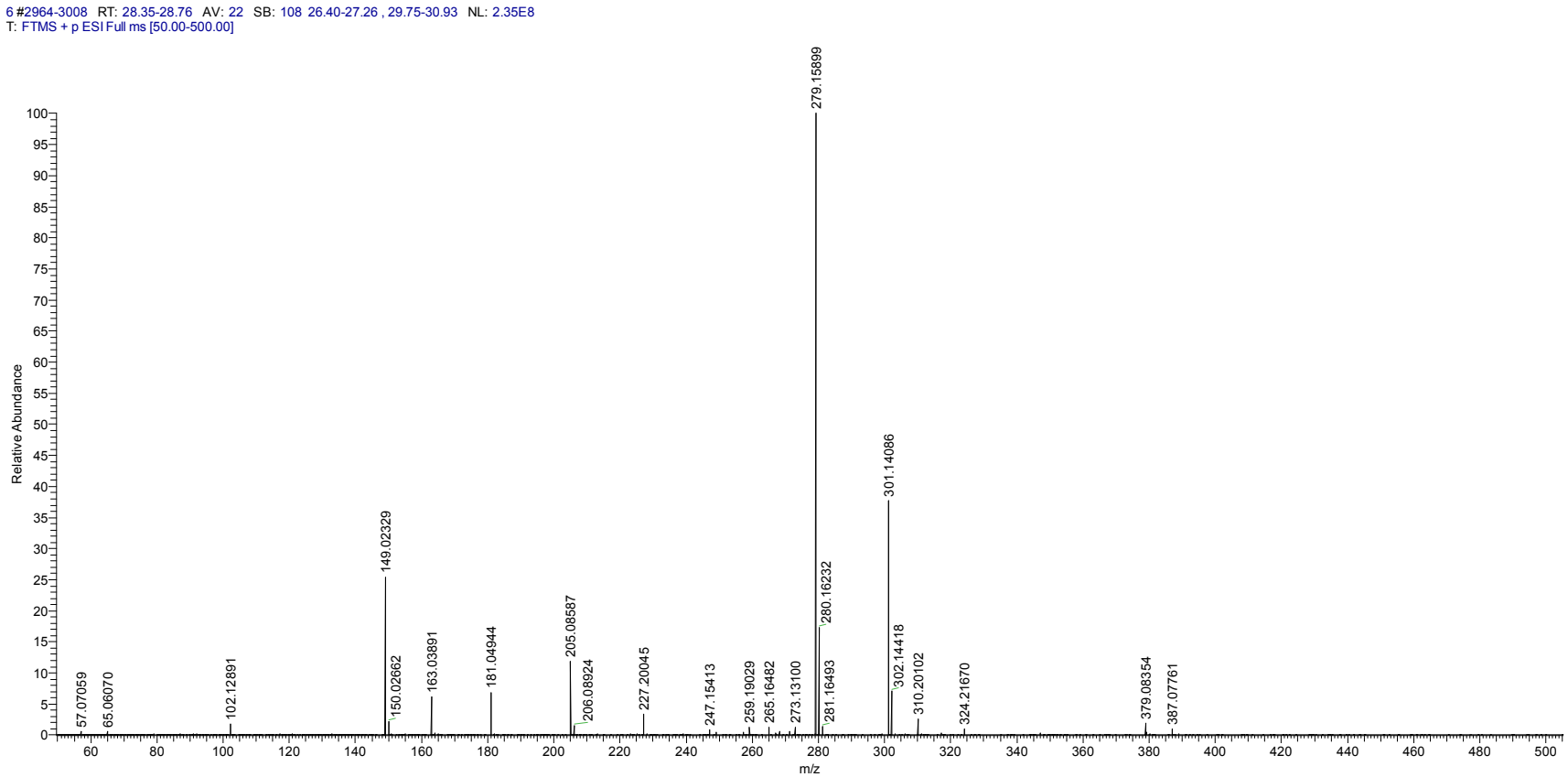

Figure S10. Mass spectra detected during the photodegradation of KET by Ag_3PO_4/P-g-C_3N_4 composite under visible light irradiation.

Table S1. The dosage of reagents used for the preparation of Ag_3PO_4 and Ag_3PO_4/P-g-C_3N_4.

Photocatalysts	P-g-C_3N_4 (mg)	$AgNO_3$ (g)	Na_2HPO_4 (mol·L^{-1})
Ag_3PO_4/P-g-C_3N_4(1:10)	500	0.0609	0.0024
Ag_3PO_4/P-g-C_3N_4(1:5)	500	0.1216	0.0048
Ag_3PO_4/P-g-C_3N_4(1:2)	500	0.3044	0.0119
Ag_3PO_4/P-g-C_3N_4(1:1)	500	0.6087	0.0239
Ag_3PO_4/P-g-C_3N_4(2:1)	250	0.6087	0.0239
Ag_3PO_4/P-g-C_3N_4(5:1)	100	0.6087	0.0239
Ag_3PO_4/P-g-C_3N_4(10:1)	100	1.2175	0.0478
Ag_3PO_4	0	1.0182	0.0400

Table S2. Electrical energy per order of the synthesized samples.

Photocatalysts	Lamp (kW)	k (min^{-1})	volume (L)	E_{EO} ($kWh \cdot m^{-3} order^{-1}$)
P-g-C_3N_4	0.8	0.00529	0.05	116144
A/CN(1:10)	0.8	0.00597	0.05	102915
A/CN(1:5)	0.8	0.00992	0.05	61935
A/CN(1:2)	0.8	0.01162	0.05	52874
A/CN(1:1)	0.8	0.03259	0.05	18852
A/CN(2:1)	0.8	0.02406	0.05	25536
A/CN(5:1)	0.8	0.02856	0.05	21513
A/CN(10:1)	0.8	0.01524	0.05	40315
Ag_3PO_4	0.8	0.01157	0.05	53103

Table S3. Water quality parameters of different water matrices.

Parameters	Milli-Q water	Tap water	Secondary Effluent water	Surface water
T(^{o}C)	24.40	22.00	26.20	28.60
pH	6.93	7.57	7.73	8.08
DO(mg·L^{-1})	5.85	6.93	5.38	6.02
ORP(mV)	35.00	26.80	-39.00	-57.00
Conductivity (μS·cm^{-1})	2.90	346.00	980.00	562.00
TDS (mg·L^{-1})	0.73	228.35	526.71	879.14

Table S4. The possible degradation intermediates of KET over Ag_3PO_4/P-g-C_3N_4 composite under visible light irradiation.

Name	m/z	Retention Time (min)	Structural Formula
P1	224	22.37	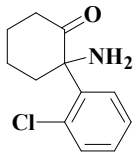
P2	222	22.37	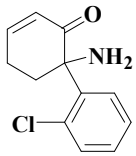
P3	236	23.90	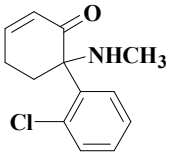
P4	254	18.87	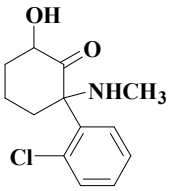
P5	256	18.87	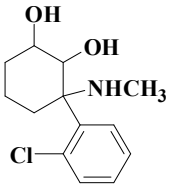
P6	200	25.85	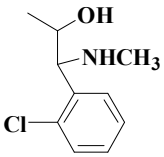
P7	240	11.86	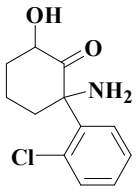

P8	225	21.14	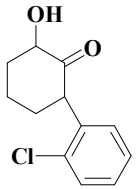
P9	226	21.14	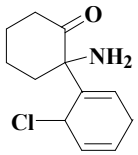
P10	243	21.14	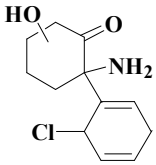
P11	241	11.86	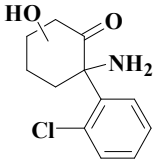
P12	279	28.16